Office of Naval Research
Department of the Navy
Contract Nonr-220(28)

UNIFORM DISTRIBUTIONS OF SOUND SOURCES ON THE SURFACE OF A RIGID SPHERE AND SOME APPLICATIONS

by

Robert Hickling

Engineering Division
CALIFORNIA INSTITUTE OF TECHNOLOGY
Pasadena, California

Report No 85-18
February 1961

Approved by:
M. S. Plesset

Office of Naval Research
Department of the Navy
Contract Nonr-220(28)

UNIFORM DISTRIBUTIONS OF SOUND SOURCES ON THE SURFACE OF A RIGID SPHERE AND SOME APPLICATIONS

Robert Hickling

Engineering Division
California Institute of Technology
Pasadena, California

Report No. 85-18
February, 1961

Approved by:
M. S. Plesset

UNIFORM DISTRIBUTIONS OF SOUND SOURCES ON THE SURFACE OF A RIGID SPHERE AND SOME APPLICATIONS

Robert Hickling*

California Institute of Technology
Pasadena, California

ABSTRACT

A study is made of certain elementary source distributions on the surface of a rigid sphere for a fairly extensive range of frequencies. The elementary systems considered consist of a point source, uniformly vibrating caps and rings, and plane line sources. Results are given for typical cases of the far zone sound fields and acoustic impedances of caps and rings, and also for the far zone sound field of a particular plane line source. Combinations of the elementary rings and caps are examined with a view to producing desired directional patterns and the results for a particular directional beam are presented. Taking a sphere as a model for the human head, the results for a point source are used to examine possible mechanisms for the binaural localization of sources of sound. These results indicate that, due to non-linear variation of phase with frequency, a pulsed sound should appear in a somewhat different form at each ear. It is suggested that localization is achieved by the brain in reconciling such pulse forms and that time and intensity differences are elements in a much more general process. Another possible application of the results involves the particular line source considered which could be taken to represent a human mouth.

---

* International Nickel Co., Inc. Fellow

1. Introduction

Most of the available theoretical information about the acoustic radiation generated by sources of finite extent concerns pistons set in a plane infinite baffle. The case of a piston set in a rigid sphere has also been treated,[1] but the sound field has not been considered in great detail.

This paper presents results of calculations carried out on a high-speed computer for certain source distributions set in the surface of a rigid sphere, namely for uniformly vibrating spherical caps (pistons) and rings, and for plane line sources of constant strength. These elementary distributions can be superimposed to give more complicated systems. Radiation impedances are computed as well as the sound fields in the far zone.

The sphere has often been used as a model for the human head. Since the principle of reciprocity equates the pressure field in the far zone due to a point source set in the sphere to the pressure distribution over the sphere due to a point source at infinity, some of the results of this paper can be considered to apply to hearing. A line source could also be taken to represent a human mouth speaking.

2. Mathematical Formulas and Calculation Procedure

The spherical polar coordinate system is used which is related to a Cartesian system having the z-axis as the polar axis, by the relations

$$\begin{aligned} x &= r \sin \phi \sin \theta \\ y &= r \cos \phi \sin \theta \\ z &= r \cos \theta \end{aligned} \qquad (1)$$

---

[1] P.M. Morse, Vibration and Sound, (McGraw-Hill Book Company, Inc., New York, 1948) pp. 321-326, 354-357.

The center of the sphere, which is of radius a, coincides with the origin of the coordinate system. The sphere is immersed in a limitless fluid and its surface is assumed to vibrate continuously with a velocity of the general form $U(\theta, \phi) \exp(-i\omega t)$, where t is the time, c is the sound velocity, λ the wavelength, $k = 2\pi/\lambda$, and $\omega = kc$.

$U(\theta, \phi)$ can be expressed in terms of spherical harmonics[2]

$$U(\theta, \phi) = \sum_{m,n} \left[A_{mn} Y^{e}_{mn}(\theta, \phi) + B_{mn} Y^{o}_{mn}(\theta, \phi) \right] \tag{2}$$

where

$$A_{mn} = \frac{(2n+1)}{4\pi} \varepsilon_m \left[\frac{(n-m)!}{(n+m)!} \right] \int_0^{2\pi} d\phi \int_0^{\pi} U(\theta, \phi) Y^{e}_{mn} \sin\theta \, d\theta \tag{3}$$

and the expression for B_{mn} is similar to that for A_{mn} except that Y^{o}_{mn} is substituted for Y^{e}_{mn}. Y^{e}_{mn} and Y^{o}_{mn} are defined as follows:

$$\begin{aligned} Y^{e}_{mn} &= \cos(m\phi) P^{m}_{n}(\cos\theta) \\ Y^{o}_{mn} &= \sin(m\phi) P^{m}_{n}(\cos\theta) \end{aligned} \qquad m \leq n \tag{4}$$

where P^{m}_{n} is the unnormalized modified Legendre function. ε_m is unity when $m = 0$, and is equal to 2 otherwise.

The resulting outgoing pressure waves in the fluid can be expressed in the form,

$$p = \sum_{m,n} \left[C_{mn} Y^{e}_{mn}(\theta, \phi) + D_{mn} Y^{o}_{mn}(\theta, \phi) \right] h_n(kr) \exp(-i\omega t) \tag{5}$$

---

[2] P. M. Morse and H. Feshbach, Methods of Theoretical Physics (McGraw-Hill Book Company, Inc., New York, 1953) Vol. II, p. 1265.

and the corresponding radial velocity can be determined by using the formula

$$u_r = - \frac{i}{\rho c} \frac{\partial p}{\partial r} \tag{6}$$

ρ being the density of the fluid. When $r = a$, u_r is equal to the velocity on the surface of the sphere given by Eq. (2), so that it follows that

$$C_{mn} = \frac{A_{mn} \rho c}{i h_n'(ka)} ; \qquad D_{mn} = \frac{B_{mn} \rho c}{i h_n'(ka)} . \tag{7}$$

The h_n' are the derivatives with respect to the argument of the spherical Bessel functions of the third kind.[3]

The radiation impedance is given by

$$F = \int_0^{2\pi} d\phi \int_0^{\pi} \left(\frac{p}{u_r} \right)_{r=a} a^2 \sin\theta \, d\theta = a^2 q_a \rho c \, (\theta p - i \chi p) \tag{8}$$

where p is obtained by inserting the relations (7) in Eq. (5), and $a^2 q_a$ denotes the area of the source distribution.

In the far zone, for a large distance r from the sphere

$$h_n(kr) \sim \exp(ikr) \, i^{-(n+1)} / r$$

and hence in this region

$$p = \rho c \, U_o (a/r) \exp \left[ik(r - ct) \right] \psi(\theta, \phi) \tag{9}$$

where

$$\psi(\theta, \phi) = \frac{1}{kaU_o} \sum_{m,n} \frac{1}{i^{n+2}} \frac{1}{h_n'(ka)} \left[A_{mn} Y^e_{mn}(\theta, \phi) + B_{mn} Y^o_{mn}(\theta, \phi) \right] \tag{10}$$

---

[3] ibid, p. 1573.

ψ, θp, χp have then to be determined over a range of ka for different forms of vibration of the surface of the sphere. If the vibrations are axisymmetric, then the solutions are independent of ϕ. m is then zero, and it follows that

$$B_{mn} = 0$$

$$Y^{e}_{on} = P_n(\cos\theta)$$

$$A_{on} = (n + \tfrac{1}{2}) \int_{o}^{\pi} U(\theta)\, P_n(\cos\theta) \sin\theta \, d\theta \qquad (11)$$

where P_n is a Legendre polynomial. If the amplitude of the vibrations has a constant value U_o over a certain axisymmetric region $\theta_1 < \theta < \theta_2$ and is zero elsewhere, then

$$A_{on} = (n + \tfrac{1}{2})\, U_o \int_{\theta_1}^{\theta_2} P_n(\cos\theta) \sin\theta \, d\theta$$

$$= \tfrac{1}{2} U_o \left\{ \left[P_{n+1}(\cos\theta_1) - P_{n-1}(\cos\theta_1) \right] + \left[P_{n-1}(\cos\theta_2) - P_{n+1}(\cos\theta_2) \right] \right\} \qquad (12)$$

where P_{-1} is taken to be unity. This corresponds to a uniformly vibrating ring set in the surface of a rigid sphere. When $\theta_1 = 0$, the case of a uniformly vibrating spherical cap or piston is obtained and

$$A_{on} = \tfrac{1}{2} U_o \left[P_{n-1}(\cos\theta_2) - P_{n+1}(\cos\theta_2) \right] . \qquad (13)$$

If in addition θ_2 is made to tend to a small quantity, say $\triangle/a$, then (13) tends to the case of a point source set in a rigid sphere,[1] namely

$$A_{on} = \tfrac{1}{2} U_o (n + \tfrac{1}{2}) \left(\frac{\triangle}{a} \right)^2 . \qquad (14)$$

For the above cases (12)-(13), the radiation impedance is determined from

$$\theta_p - i\chi_p = \left[\frac{1}{2(\cos\theta_1 - \cos\theta_2)}\right] \sum_n \left[\frac{h_n(ka)}{ih'_n(ka)}\right] \frac{1}{(2n+1)} \left[\frac{A_{on}}{U_o}\right]^2 . \qquad (15)$$

When the surface vibrations are not axisymmetric the problem becomes more complicated, but certain examples can still be solved relatively easily. Consider a section of the uniformly vibrating ring already discussed, for values of ϕ lying between $\pm\phi_1$, with all the remainder of the surface held rigid. Since

$$\int_{-\phi_1}^{\phi_1} \sin(m\phi)\, d\phi = 0$$

$$\int_{-\phi_1}^{\phi_1} \cos(m\phi)\, d\phi = 2\sin(m\phi_1)/m \quad ; \qquad m > 0$$

$$= 2\phi_1 \quad ; \qquad m = 0$$

it follows that

$$B_{mn} = 0$$

$$A_{mn} = \frac{(2n+1)}{m\pi} U_o \left[\frac{(n-m)!}{(n+m)!}\right] \sin m\phi_1 \int_{\theta_1}^{\theta_2} P_n^m(\cos\theta) \sin\theta\, d\theta \qquad m > 0$$

$$A_{on} = \frac{(2n+1)}{2\pi} U_o \phi_1 \int_{\theta_1}^{\theta_2} P_n(\cos\theta) \sin\theta\, d\theta .$$

If $\theta_2 = \theta_1 + \Delta\theta$ where $\Delta\theta$ is small, then

$$A_{mn} = \frac{(2n+1)}{m\pi} U_o \triangle\theta \left[\frac{(n-m)!}{(n+m)!}\right] \sin m\phi_1 P_n^m(\cos\theta_1) \sin\theta_1 \qquad m > 0$$

$$A_{on} = \frac{(2n+1)}{2\pi} U_o \triangle\theta \, \phi_1 P_n(\cos\theta_1) \sin\theta_1 \, . \qquad (16)$$

This is the case of a plane line source embedded in the surface of a rigid sphere. The radiation impedance cannot be determined as in Eq. (15) because the corresponding series does not converge.

For ease in calculation the modified Legendre polynomials were expressed in the semi-normalized form

$$\overline{P}_n^m = \left[\frac{(n-m)!}{(n+m)!}\right]^{1/2} P_n^m \, . \qquad (17)$$

Since it was necessary to have P_n, and P_n^m to very high orders (n, m about 40), the calculations had to be carried out in double precision.

The Bessel function subroutine which was carried out in single precision achieved an accuracy of about six figures in the range up to $n = 35$ when compared with standard tables.[4] A check on the derivatives showed a similar accuracy.

The sound pressure in the far zone given by the function ψ of Eq. (10) was obtained for a range of ka from 1 to 25 for the following source distributions:

(a) a point source;

(b) uniformly vibrating spherical caps for θ extending over the regions defined by: 0^o - 20^o, 0^o - 40^o, 0^o - 60^o ;

(c) individual uniformly vibrating rings for θ in the regions defined by: 20^o - 25^o, 40^o - 45^o, 60^o - 65^o ;

---

[4] Mathematical Tables Project of the National Bureau of Standards; Tables of Spherical Bessel Functions, Vols. I and II (New York, Columbia University Press, 1947)

(d) a uniform line source situated along $\theta_1 = 45^\circ$, between the limits $\phi_1 = \pm 10^\circ$.

The results are presented in the form of the argument and modulus of ψ in Figs. 1-9. The modulus, of course, is the absolute value of the sound pressure in the far zone. The individual lines in the figures represent the variation with respect to ka at a particular point in the far zone sound field defined by the coordinates (θ, ϕ). The sound field for any particular frequency is thus obtained by reading off the values where the ordinate at that frequency intersects the lines. The argument of ψ could not be presented more accurately, since in general it changes quite rapidly over the range of ka considered. However, it can at least be shown how it changes qualitatively with changes in source configuration.

The impedances θp, χp were determined for a variety of rings and caps using Eq. (15) and are presented in Figs. 10 and 11.

The results of supplementary calculations are given in Figs. 12-17 and are described in the next sections.

3. Discussion of Results

Figure 1 gives the far zone pressure field* for a point source set in the surface of a rigid sphere. At very low frequencies, the sound is radiated uniformly in all directions. At very high frequencies, the sound is also radiated uniformly, but only into the half space tangential to the sphere at the point source. This is because the dimensions of the point source have been assumed to be much smaller than any given value of the wavelength. The variation of phase with frequency is linear as shown in

---

* The results for the pressure amplitude agree in general with those given in Fig. 66, ref. 1.

Fig. 1(b). At low frequencies, below about ka = 1.5, the lines are not quite straight, but curve to a phase value of 90° at ka = 0. This is shown in Fig. 14. The initial slope for $ka << 1$ agrees with the relation[1] $-\frac{3}{2}\cos\theta/\left[1 + (\frac{3}{2}ka\cos\theta)^2\right]$.

Due to the principle of reciprocity[1] the pressure field in the far zone is proportional to the pressure distribution over a rigid sphere due to a point source at infinity. The factor of proportionality is i/ka, so that to obtain the solution of this problem from Fig. 1, the modulus of ψ is divided by ka. The phase remains the same except that the coordinate system is shifted vertically so that the origin coincides with the focus of the straight lines. The application of these results to binaural localization of sound will be discussed in the next section.

Figures 2-4 show the development of the sound field as the spherical cap changes size. As usual at the low frequency limit, the radiation is uniform in all directions. At very high frequencies, the situation is not so definite. It has been shown[5] that the radiation field at very high frequencies has the same form as that of the given velocity distribution over the surface of the sphere. This tendency is apparent in the figures showing the pressure amplitude. In the far zone outside the cone defined by the cap angle, the pressure amplitude lines can be seen to be going to zero. For values of θ lying inside the cone, the lines were found to be tending to settle around $|\psi|$ equal to unity, except for points directly on the axis $\theta = 0$. This was investigated as far out as ka = 70 for caps whose half angles went over the range from 10° to 170°. Some of the $\theta = 0$ pressure amplitude curves are shown in Fig. 12. The number of oscillations about

---

[5] Morse and Feshbach, p. 1479.

the mean $|\psi| = 1$ increases very rapidly as the cap increases in size, but the amplitude decreases in size although only slowly at first. In the limit when the cap covers the entire surface of the sphere, the expected result of a constant amplitude at all frequencies is attained. For values of θ near zero the pressure amplitude at first follows the $\theta = 0$ curve quite closely, but at very high frequencies it begins to settle down around $|\psi| = 1$. Hence, although according to calculation the oscillatory nature of the $\theta = 0$ pressure amplitude persists at very high frequencies, it will eventually have no existence in any physical sense.

As the cap decreases in size the radiation field resembles that of a point source over an increasingly greater part of the frequency range. However the behavior at high frequencies is eventually the same, because the wavelengths become much smaller than the dimensions of the cap.

The behavior of rings is similar to that of caps at the high and low ends of the frequency range. At the low frequencies the radiation is uniform and at very high frequencies all the radiation is concentrated uniformly in the region defined by the angle subtended by the thickness of the ring. Figures 5-7 show how the sound field varies as a 5° ring is moved backwards over the sphere. These results can also be used to analyze how the sound fields of the caps are built up as they are increased in size. For example, if the 40°-45° ring is added to the 40° cap to produce a 45° cap, then the phase difference at about $ka = 25$ is approximately 180° for the $\theta = 0$ lines. This means that the sound intensity at $\theta = 0$ will be decreased by the addition of the ring hence assisting in the process of the formation of the rapid fluctuations shown in Fig. 12. The sound field in other directions and for other combinations of the elementary rings could be analyzed in a similar way.

The phase variation with frequency as shown in Figs. 2(b)-7(b) indicates some general tendencies. As the cap grows larger or as the ring is moved backwards over the sphere the rate of change of phase with frequency grows smaller. Also, as might be expected, the abrupt changes of phase which occur coincide with sharp minima in amplitude. Other trends can also be observed.

It seems likely that certain desired sound fields which are axisymmetric and fairly simple in form could be approximated by arrays of rings whose relative phases and amplitudes are chosen specifically for the purpose. For example the directional beam of Fig. 13 is obtained by combining a 40° cap with a 40°-45° ring at a frequency corresponding to $ka = 14.2$. The ring is made to vibrate 180° out of phase with the cap, while the amplitude of the caps vibrations is 1/3 that of the ring.

The acoustic impedances of the caps and rings are shown in Figs. 10 and 11. As the cap increases in size the resistive part of its impedance approaches the high frequency limit ρc more rapidly, while the reactive part has its maximum at progressively lower frequencies. Rings behave roughly in the same manner as caps which subtend the same angle at the center of the sphere. Thus 5° rings behave similarly to the 5° cap, and a 40° ring is similar in behavior to the 40° cap. The number of oscillations increases as a ring moves backwards from its initial position as cap.

Figures 8 and 9 give the far zone pressure field due to a uniform plane line source situated on the plane $\theta_1 = 45^{\circ}$ between the limits $\phi_1 = \pm 10^{\circ}$. This particular example was chosen because it might represent a model of the human mouth. Figure 8 gives the results in the meridian half plane $\phi = 0$ directly ahead of the line source and Fig. 9 in the equatorial plane $\theta = 90^{\circ}$. For higher frequencies the results in the $\phi = 0$ plane

resemble those for a point source. The intensity at $\theta = 90^{\circ}$ is of the same order as that at $\theta = 0^{\circ}$ but has developed oscillations. The effect of the length of the line source on phase shows up at lower frequencies particularly in the equatorial plane $\theta = 90^{\circ}$. In the region ahead of the line source approximately $\phi = \pm 60^{\circ}$, the phase remains roughly constant over the range of frequencies from ka = 1 to 2, and linear at higher frequencies. Outside this region the phase variation is quite disturbed. As the length of the line source is increased the results tend gradually to those for a thin ring at $\theta = 45^{\circ}$.

4. Binaural Localization of Sources of Sound

As has been pointed out in the previous section, the far zone pressure field for the point source is the same as the pressure distribution over the surface of a rigid sphere due to a point source at infinity, i.e., due to plane waves incident on the sphere. It is possible therefore to examine mechanisms for localizing a source of sound using the amplitude and phase observed at two diametrically opposite points on the surface of the sphere. Such mechanisms might then be expected to be similar to the mechanisms employed by ears set in a human head. For this purpose it is usually assumed that the head and the sphere correspond roughly in size so that the radius of the sphere will be taken to be about 3.4 inches. Hence a frequency of approximately 620 cycles will be represented by a value of ka = 1, and proportionately for any other frequency. It should be pointed out, however, that due to the symmetry of the sphere a sound source can only be located as on the surface of a cone whose axis is the diameter at the ends of which the measurements are made. In actuality sounds are localized a little more accurately by making use of the asymmetry of the head and body and the

sensations of sound experienced elsewhere than at the ears, although discrimination is well developed only in the horizontal plane.[6]

The current view held by experimenters in the field is that localization is achieved at low frequencies by making use of the phase difference between the two ears and at high frequencies by using the intensity difference. This explanation was first proposed by Rayleigh[7] although the emphasis of his conclusions was somewhat modified later.[8] The experiments which have been performed use both pulses and pure tones, the latter having to be used very carefully in order to exclude transient effects. The direction of a pulsed sound was found to be quite readily distinguished. The results for pure tones are more conflicting, but some of the more successful experiments[9] have been carried out at frequencies of only a few hundred cycles.

In order to discuss the usefulness of intensity differences, some results should be quoted. Banister[10] found that in order to achieve a sensation of deviation from the median plane an intensity difference between the ears of more than 4db was necessary. In addition, phase differences of pure tones become ambiguous above 1,200 cycles[6] (also compare Figs. 15(b), 16(b)), so that it would seem that intensity differences should be the significant factor for the higher frequencies. However if a direction of 15^{o} to the median plane be accepted[6,11] as the minimum deviation which can be readily perceived (the actual minimum angle is probably less than

---

[6] Woodworth and Schlosberg: Experimental Psychology (Henry Holt and Co., New York, 1955) pp. 349-361.

[7] Rayleigh: Theory of Sound (Dover Publications, New York, 1945), Vol. II, pp. 442-3.

[8] Rayleigh: Phil. Mag. (6) 13, 214, (1907).

[9] J. R. Pierce: Some Work on Hearing, American Scientist, Vol. 38, 1, p. 40, March 1960.

[10] H. Banister: Brit. Journ. of Psych. 16, 265, 1926.

[11]

half this amount), then on the basis of Banister's findings, the results for a sphere show that intensity differences can never be of sufficient significance in determining the direction of a distant source of sound. For example, in Fig. 16(a) (which gives the pressure distribution over the sphere when the frequency is about 6,200 cycles) for a source situated 15° from the median plane at $\theta = 90^{\circ}$, the ratio of the pressure amplitudes would be 3.95/2.55, an intensity difference somewhat less than 4db. Figure 1 does not hold out the possibility of improvement at higher frequencies. At very high frequencies it is clear that not much discrimination can be expected when one side of the sphere is equally illuminated and the other side equally in a shadow. For an actual head, it is clear that the pinna must play a role at higher frequencies, but it also seems apparent that over a wide section of the audible frequency range, intensity differences will at best be only marginally significant for a distant source of sound. This conclusion appears to be in contradiction to the known fact that intensity differences produce a sensation of "sidedness" or deviation from the median plane. However, it is apparent that larger intensity differences will occur when the deviations from the median are more than 15° so that a less accurate localization of distant sources of sound is still possible by means of intensity differences. Larger intensity differences are also obtained when the sound source is brought closer to the head. For example, Figure 17 which is obtained from the general Eq. (5), shows that for a 15° deviation the intensity difference for a tone of approximately 6,200 cycles is increased to a maximum of about 8db as the source approaches the head. The distance at which the intensity difference rises to a sufficient degree above the 4db threshold is not very certain, but it seems to be only a few feet at the most. Similar results hold down to about 2k/cs. It would seem,

therefore, that the higher frequency pure tones cannot be localized very accurately by means of intensity differences unless the source is within a few feet of the head.

This conclusion has a bearing on the localization of pulsed sounds. As has already been stated, a pulsed sound can be localized very readily at all distances - certainly within the 15^{o} deviation which has been set up as a criterion. In view of the apparent inaccuracy in localizing the constituent tones in the higher frequency range, it might be expected that additional properties inherent in the nature of a pulse are responsible for this enhanced ability. A pulse can be analysed by using the results in Fig. 1 (with the amplitude divided by ka) which indicates how the amplitude and phase in the pulse will vary with frequency when the sound source is more than several feet away. Because of previous conclusions on intensity differences, it does not appear that amplitude variation will play a significant role. The phase variation with frequency is seen to be linear above about 1,500 cycles each direction having a certain fixed slope, and this linearity provides a localization mechanism which has often been suggested for pulses, namely a difference in arrival time of the pulse at each ear. As might be expected, the differences in arrival time computed from Fig. 1(b) agree very well with the results given by Woodworth and Schlosberg[6], who use a simple path difference theory valid only for higher frequencies. The formula, therefore, which would give the phase difference between the ears in this range is of the form

$$\text{phase difference} = ka(\theta_d + \sin\theta_d) \tag{18}$$

where θ_d is the angle which the incident sound waves make with the median plane at $\theta = 90^{o}$. The arrival time differences can be readily

determined from this formula. From the results, it appears that the ears have to distinguish a difference of the order of 1/10 millisecond and from experiment this appears on the average to be the minimal amount required to achieve an effective sensation of "sidedness".[6,12] However there is always the problem of determining the precise arrival time of a pulse, the time differences which are used being at the most about 1 per cent of pulse length.[6] In order to obviate this difficulty, it has been suggested that the time differences which the ears sense are obtained from a continuous comparison in the arrival time of different parts of the same pulse at each ear. However it would seem that the same pulse form will not occur at each ear. As shown in Fig. 14, the change of phase with frequency is not linear over the whole frequency range. The slope changes at about 2k/cs so that the simple path difference theory breaks down when the sphere is smaller than about 1/3 the wave length of the incident waves. Hence for an actual head it would be expected that the non-linearity would persist to much higher frequencies, because the irregularities of the head and pinna provide much greater curvatures for the incident sound to contend with than the gross effect of the spherical model. Thus it would appear that a pulse would not only arrive at each ear at a somewhat time but more generally in a somewhat different form. It is known[9] that the ear is quite sensitive to changes in pulse form and hence using more general differences of this type would seem a more sophisticated mechanism for sound localization than using only time and intensity differences. To reconcile two such sensations into a single impression is not an uncommon feature in nature, so that such an idea is not in such obvious conflict with experience as it might seem.

---

[12] R. G. Klumpp, H. R. Eady: J.A.S.A., 28, 859, 1956.

The diffraction of sound around the head must surely be sufficiently complex to produce different pulse forms at each ear, thus requiring an automatic reconciliation process in the brain, and if such a reconciliation process exists it must surely be combined with the ability to localize a sound. The fact that the calculated time and intensity differences are so minimal for such a large deviation as 15^{o} certainly leaves room for such a hypothesis. Unfortunately, it cannot be indicated as yet what changes in pulse form would be significant. The ear has obviously gone through a learning process of comparable complexity to that of the eye, but as yet there appears to be no clear insight into the kinds of recognition patterns which it uses.

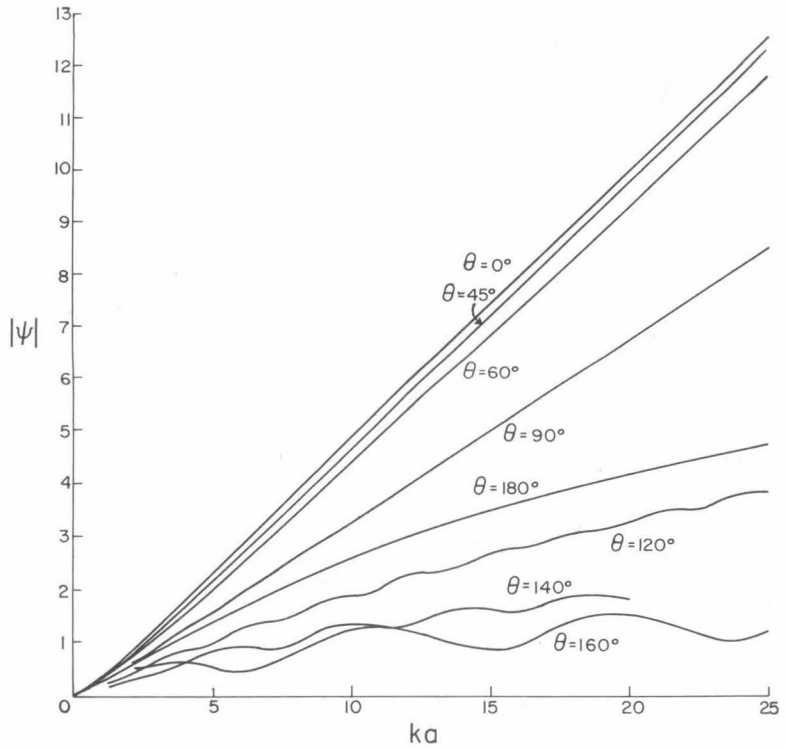

(a) The far zone pressure amplitude as a function of frequency due to a point source set in the surface of a rigid sphere.

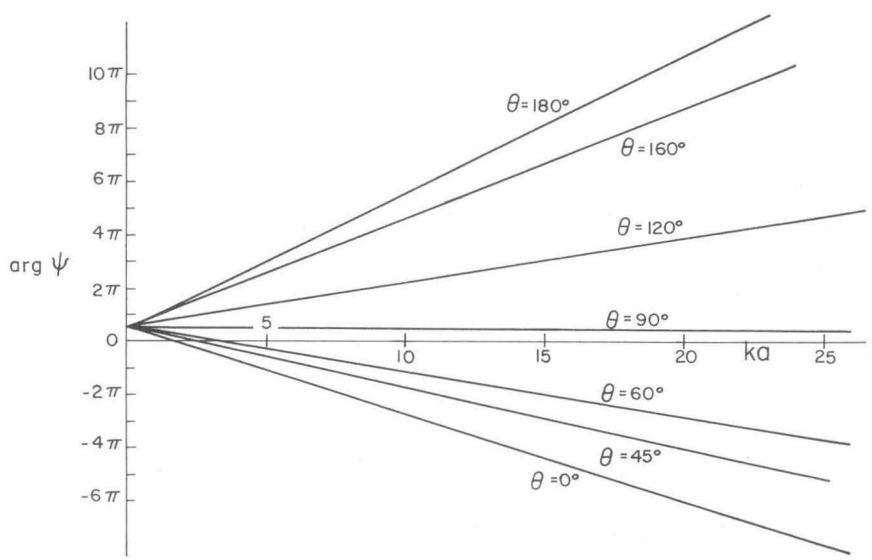

(b) The phase of the far zone pressure field as a function of frequency due to a point source set in the surface of a rigid sphere.

Fig. 1

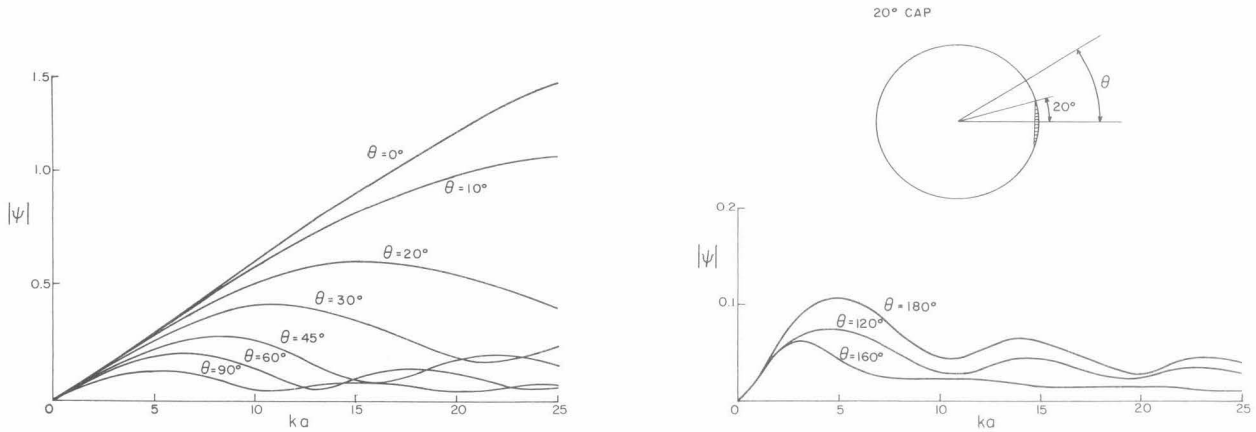

(a) The far zone pressure amplitude as a function of frequency due to a 20^{o} cap set in the surface of a rigid sphere.

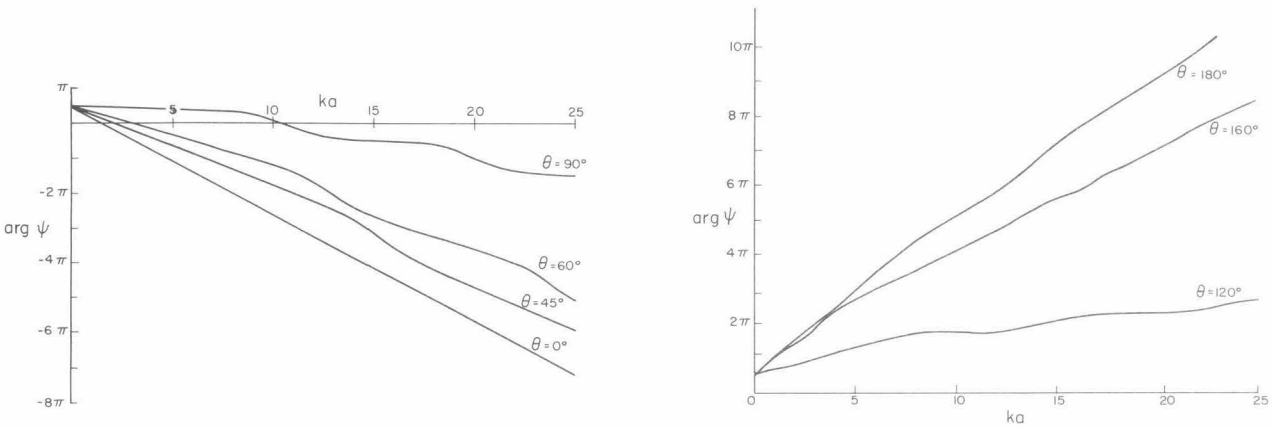

(b) The phase of the far zone pressure field as a function of frequency due to a 20^{o} cap set in the surface of a rigid sphere.

Fig. 2

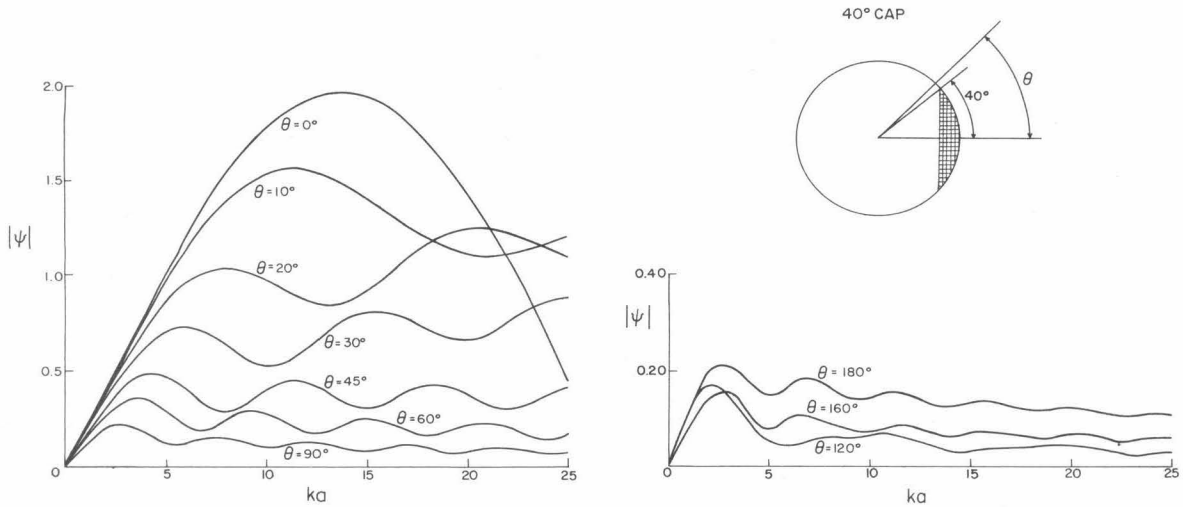

(a) The far zone pressure amplitude as a function of frequency due to a 40° cap set in the surface of a rigid sphere.

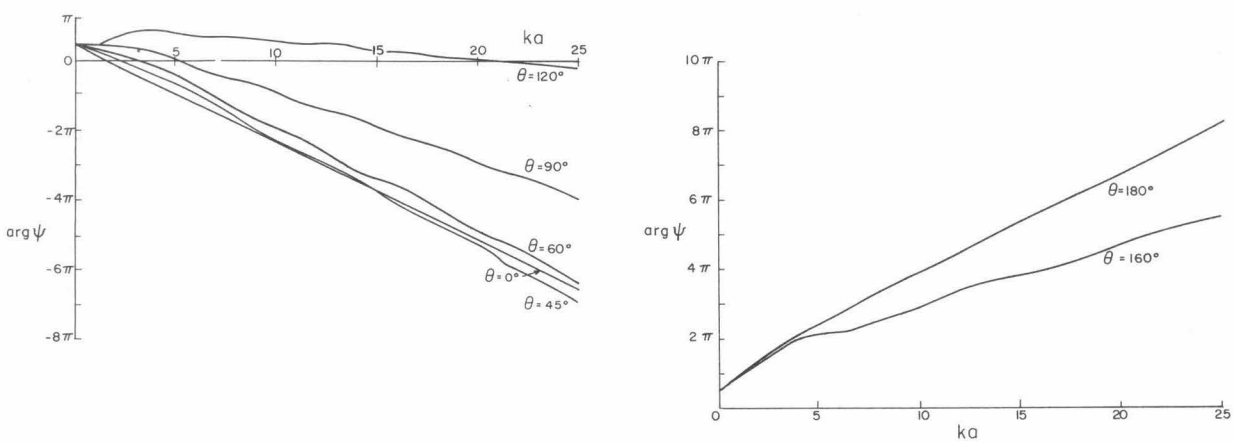

(b) The phase of the far zone pressure field as a function of frequency due to a 40° cap set in the surface of a rigid sphere.

Fig. 3

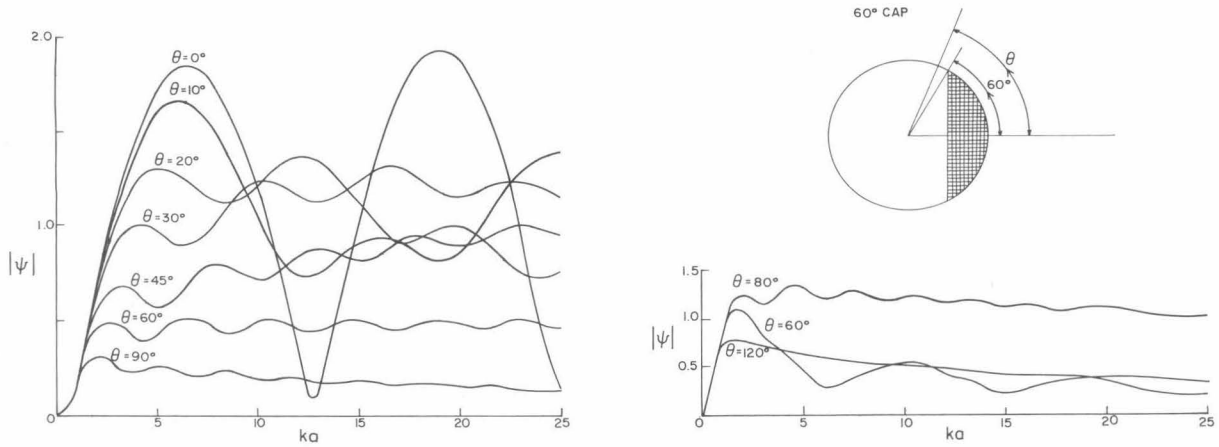

(a) The far zone pressure amplitude as a function of frequency due to a 60° cap set in the surface of a rigid sphere.

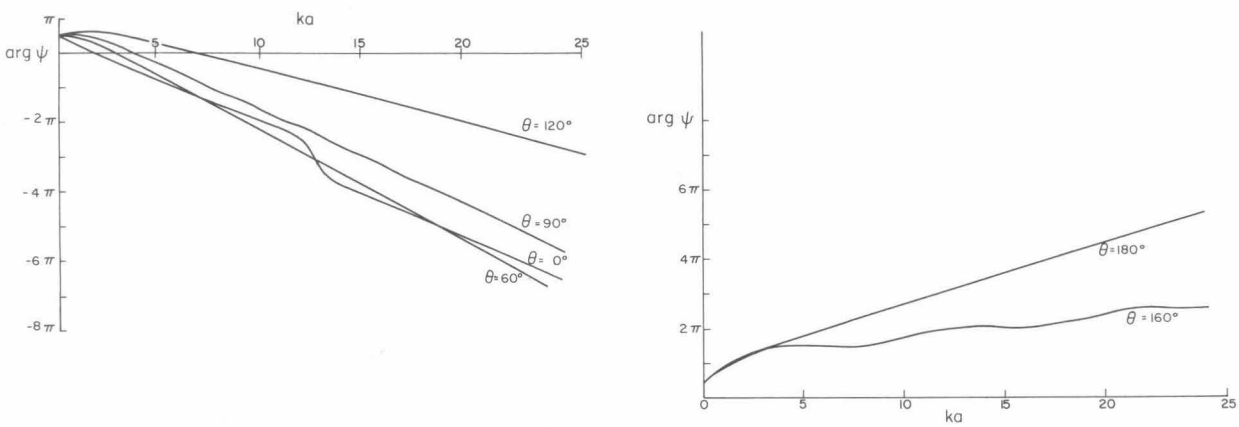

(b) The phase of the far zone pressure field as a function of frequency due to a 60° cap set in the surface of a rigid sphere.

Fig. 4

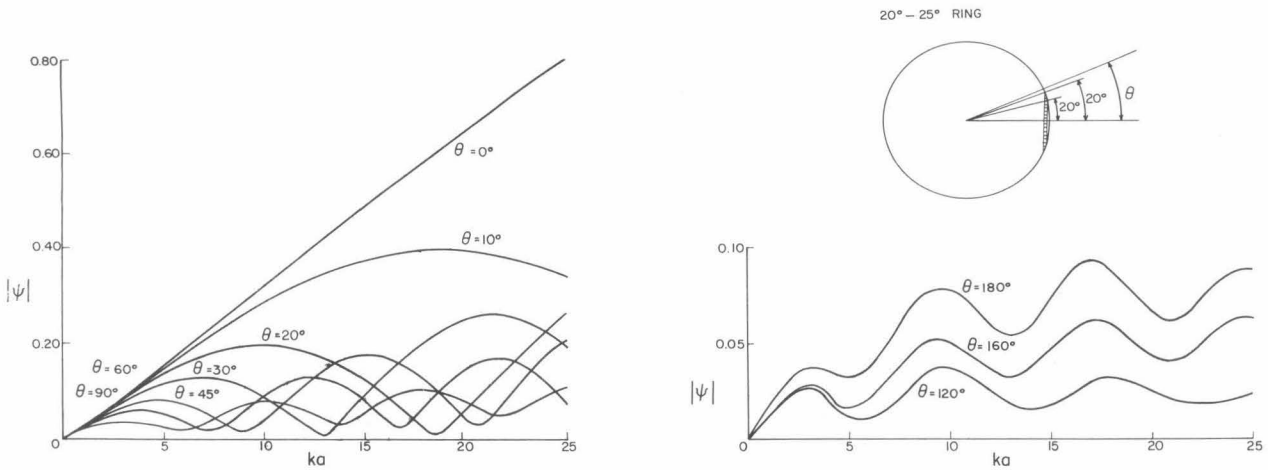

(a) The far zone pressure amplitude as a function of frequency due to a 20^{o} - 25^{o} ring set in the surface of a rigid sphere.

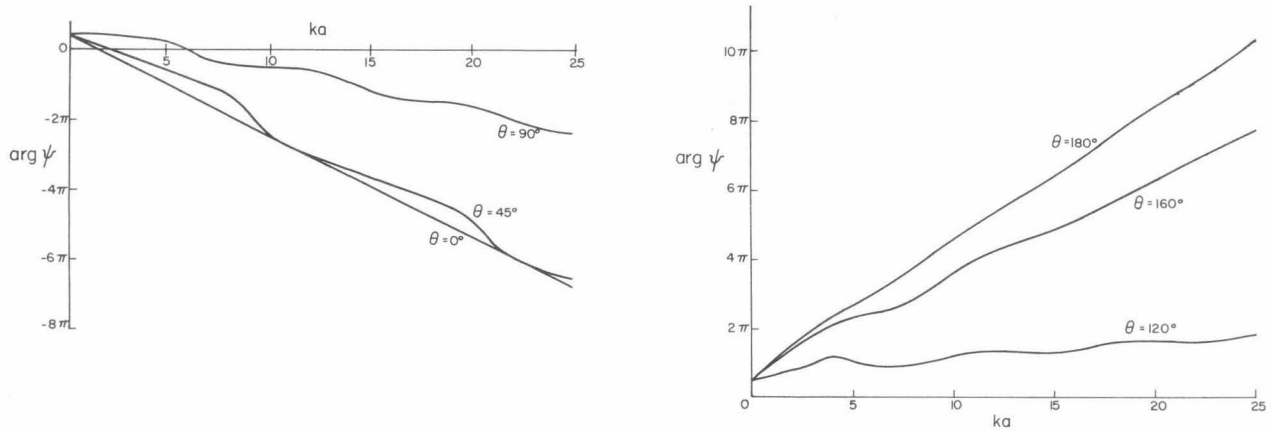

(b) The phase of the far zone pressure field as a function of frequency due to a 20^{o} - 25^{o} ring set in the surface of a rigid sphere.

Fig. 5

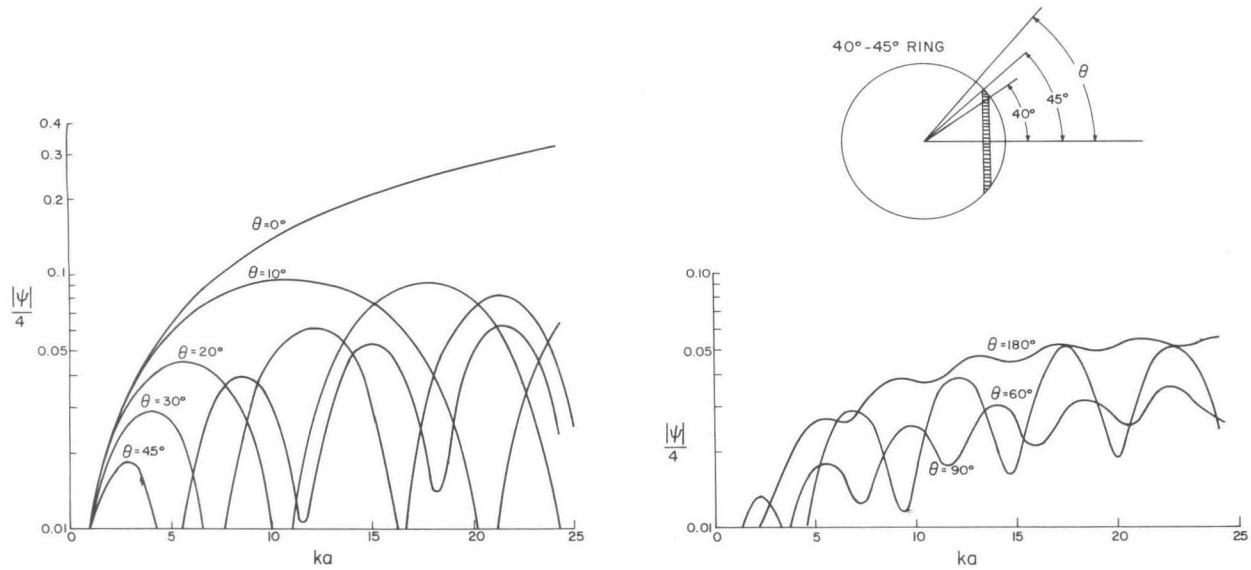

(a) The far zone pressure amplitude as a function of frequency due to a 40^{o} - 45^{o} ring set in the surface of a rigid sphere.

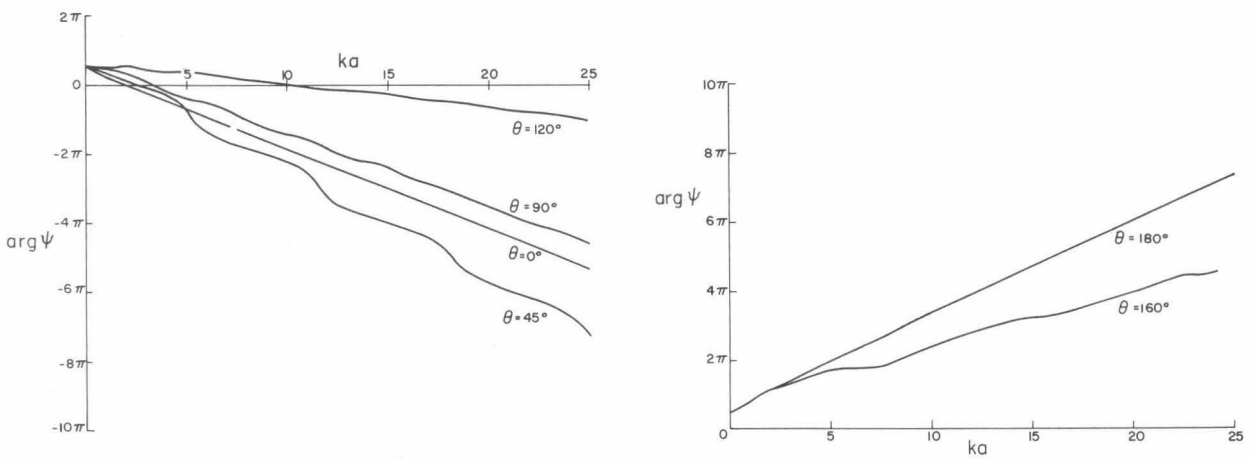

(b) The phase of the far zone pressure field as a function of frequency due to a 40^{o} - 45^{o} ring set in the surface of a rigid sphere.

Fig. 6

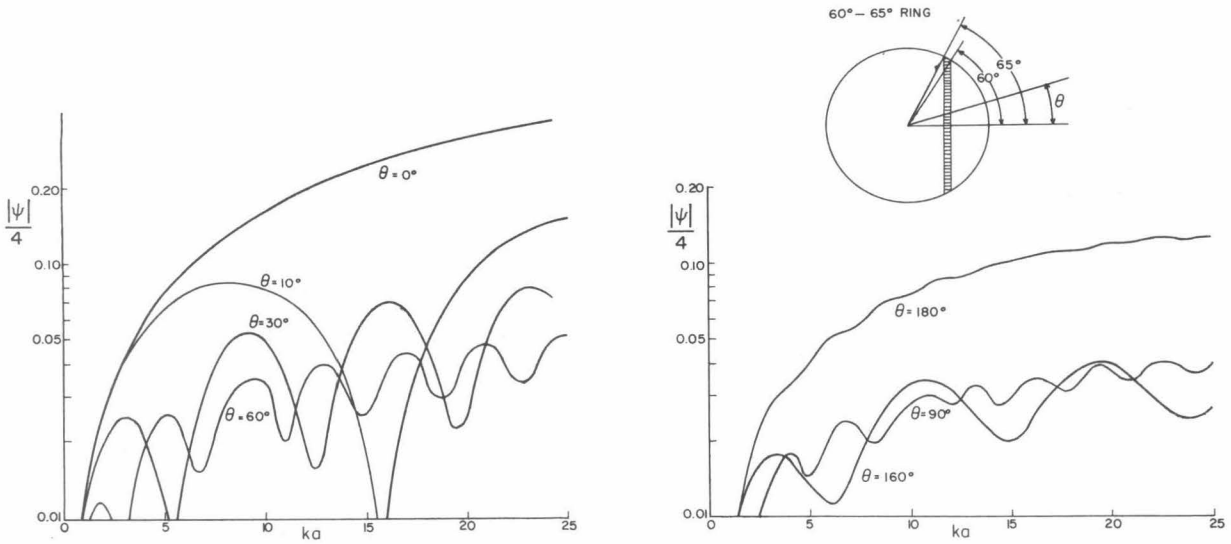

(a) The far zone pressure amplitude as a function of frequency due to a 60^{o} - 65^{o} ring set in the surface of a rigid sphere.

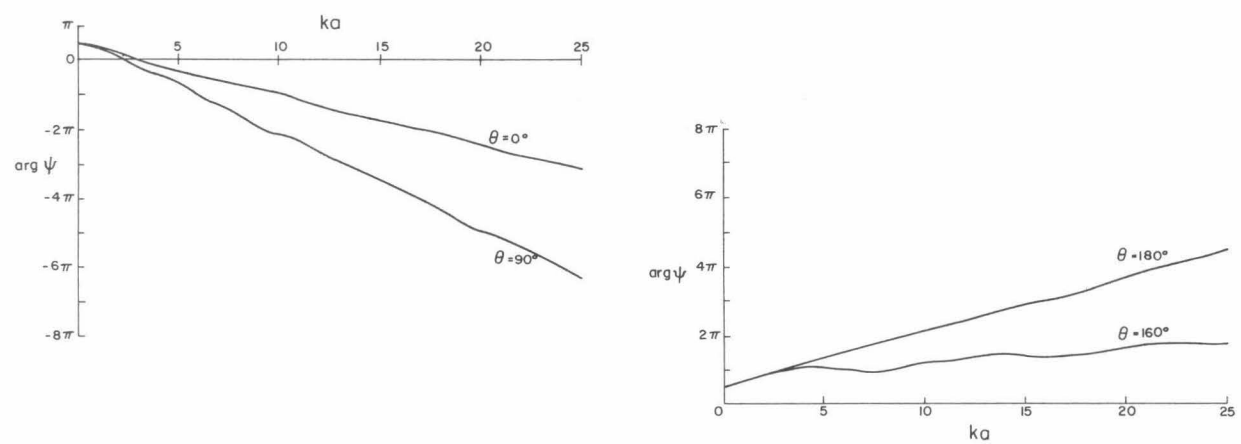

(b) The phase of the far zone pressure field as a function of frequency due to a 60^{o} - 65^{o} ring set in the surface of a rigid sphere.

Fig. 7

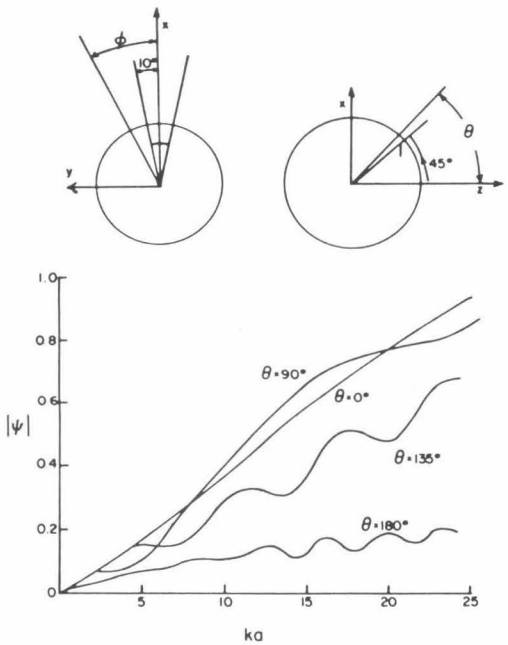

(a) The far zone pressure amplitude as a function of frequency due to a plane line source situated on the plane $\theta_1 = 45^\circ$ between the limits $\phi_1 = \pm 10^\circ$ in the surface of a rigid sphere. The section of the far zone field considered is in the meridian half plane $\phi = 0$.

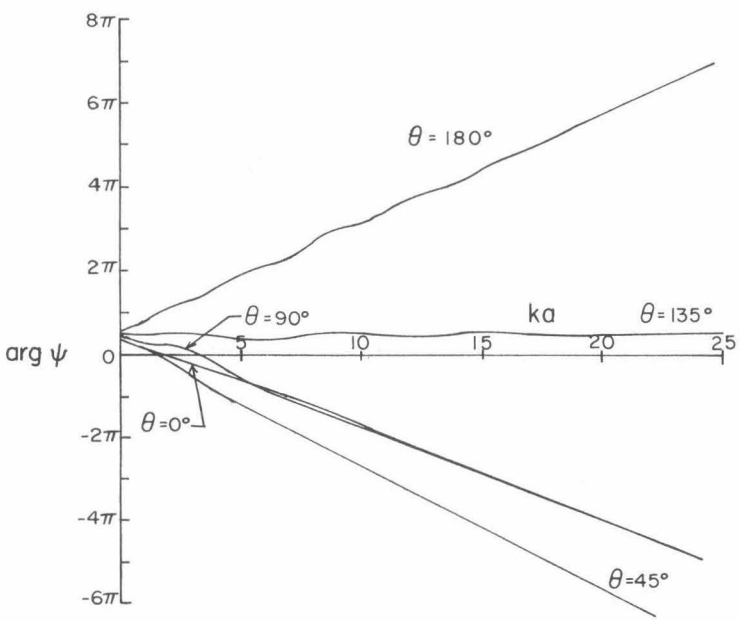

(b) The phase of the far zone pressure field as a function of frequency due to the plane line source defined by $\theta_1 = 45^\circ$, $\phi_1 = \pm 10^\circ$. The section of the far zone field considered is in the meridian half plane $\phi = 0$.

Fig. 8

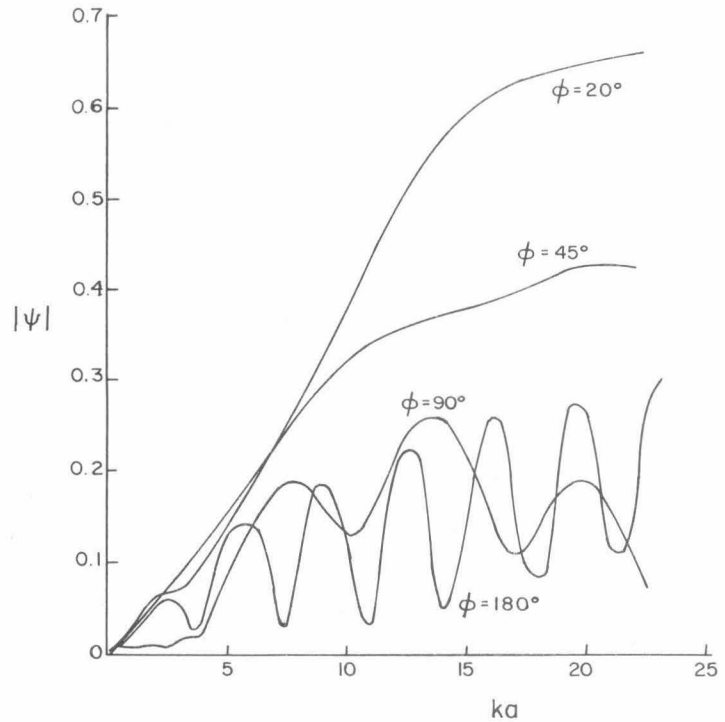

(a) The far zone pressure amplitude as a function of frequency due to the plane line source defined by $\theta_1 = 45^\circ$, $\phi_1 = \pm 10^\circ$. The section of the far zone field considered is in the equatorial plane $\theta = 90^\circ$.

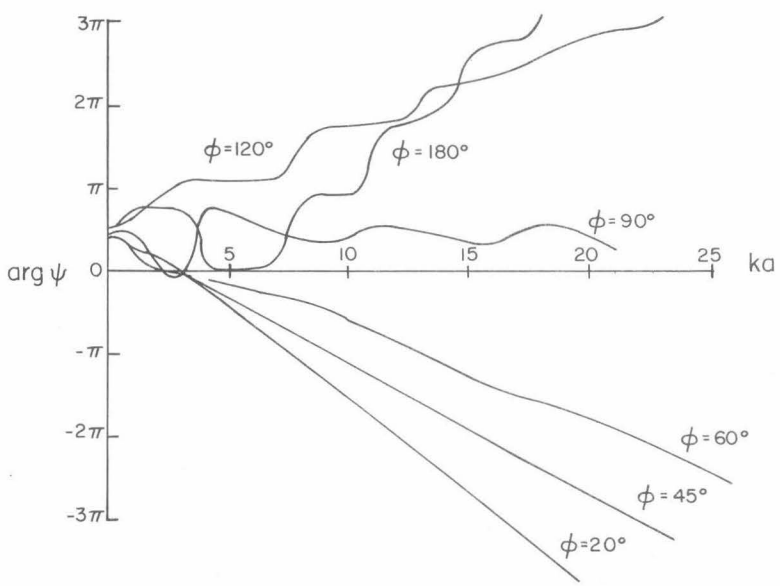

(b) The phase of the far zone pressure field as a function of frequency due to the plane line source defined by $\theta_1 = 45^\circ$, $\phi_1 = \pm 10^\circ$. The section of the far zone field considered is in the equatorial plane $\theta = 90^\circ$.

Fig. 9

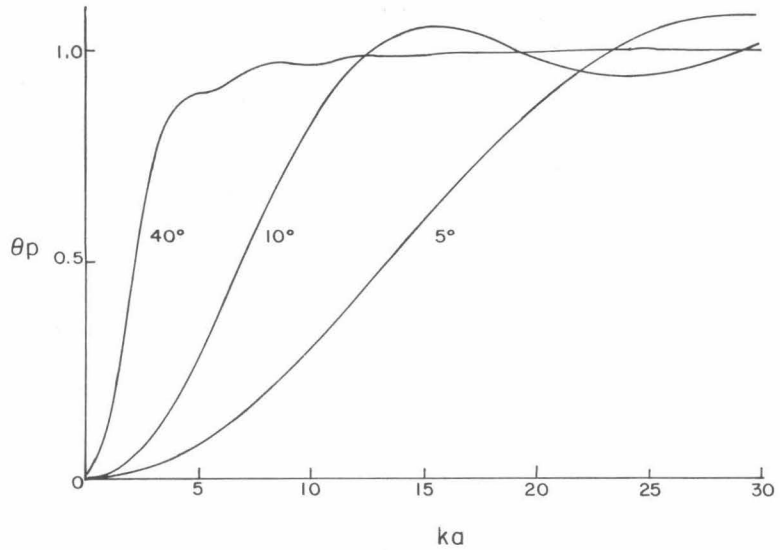

(a) Resistive part θp of the acoustic impedance of the 5°, 10°, 40° caps as a function of frequency.

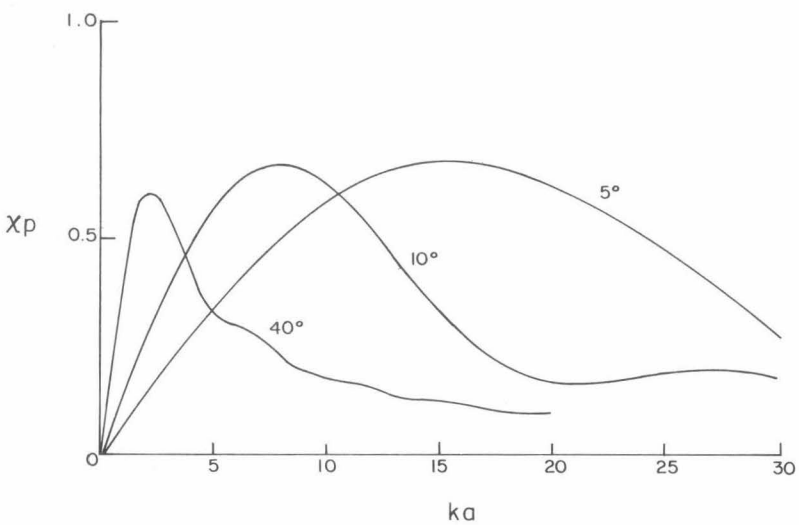

(b) Reactive part χp of the acoustic impedance of the 5°, 10°, 40° caps as a function of frequency.

Fig. 10

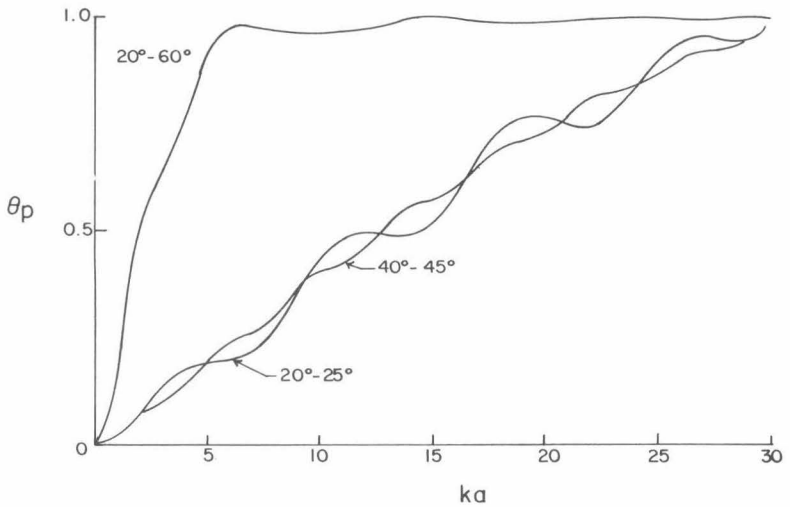

(a) Resistive part θp of the acoustic impedance of the 20° - 25°, 40° - 45°, 20° - 60° rings as a function of frequency.

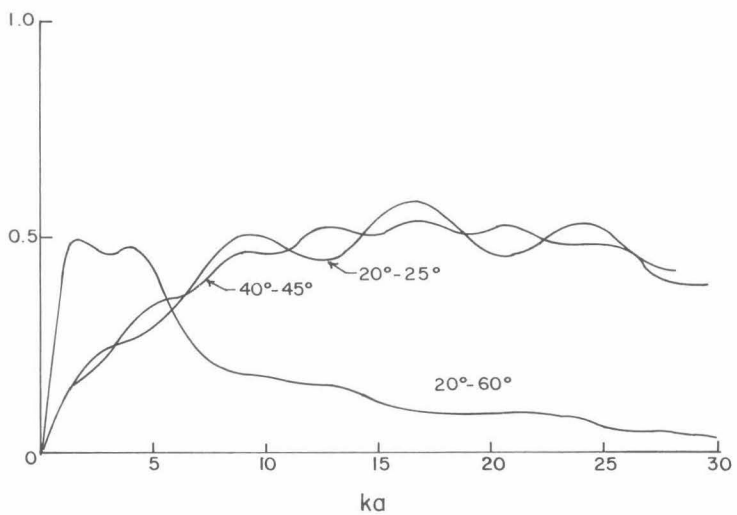

(b) Reactive part χp of the acoustic impedance of the 20° - 25°, 40° - 45°, 20° - 60° rings as a function of frequency.

Fig. 11

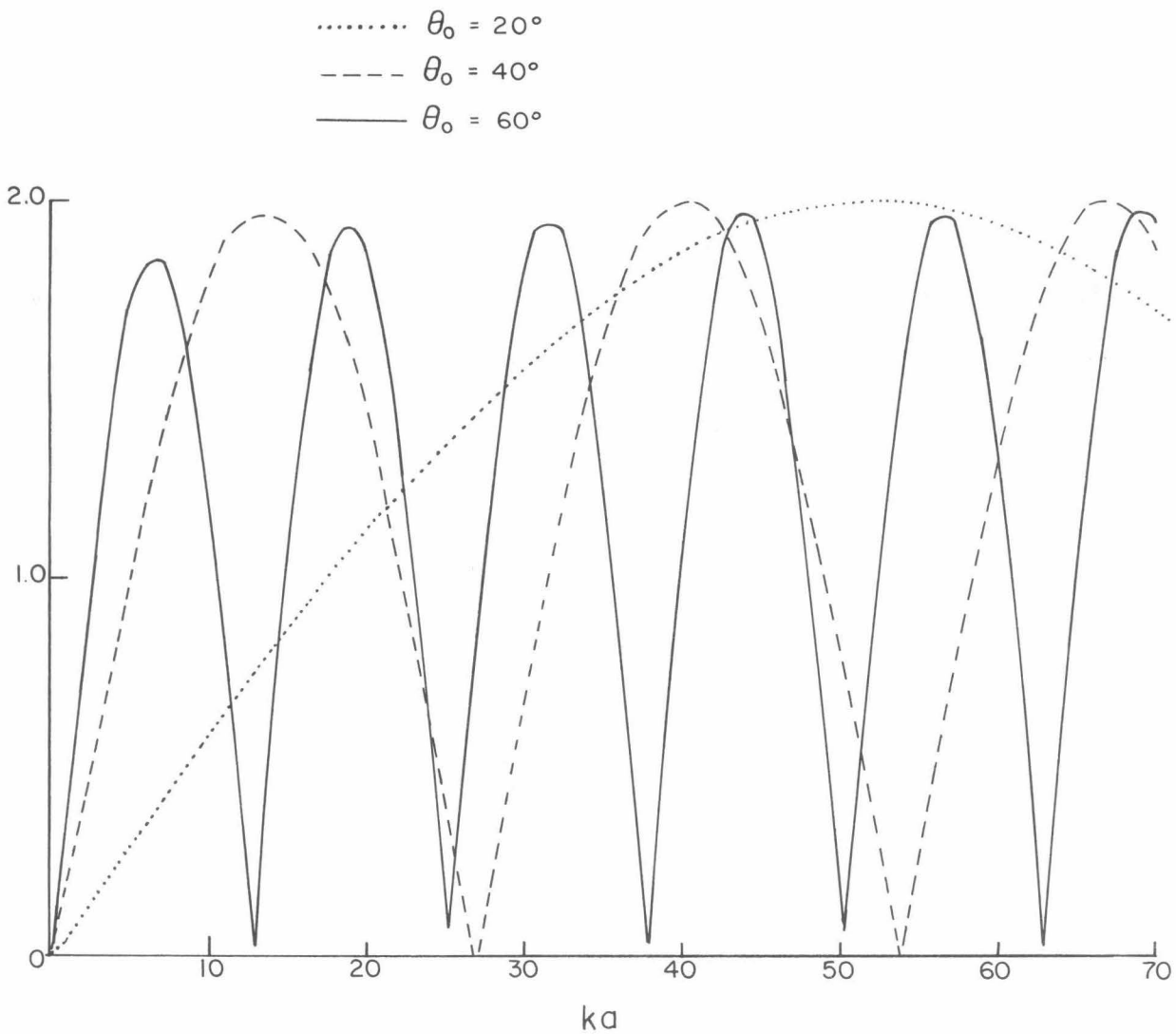

The far zone pressure amplitude on the axis $\theta = 0$ as a function of frequency for caps of increasing size.

Fig. 12

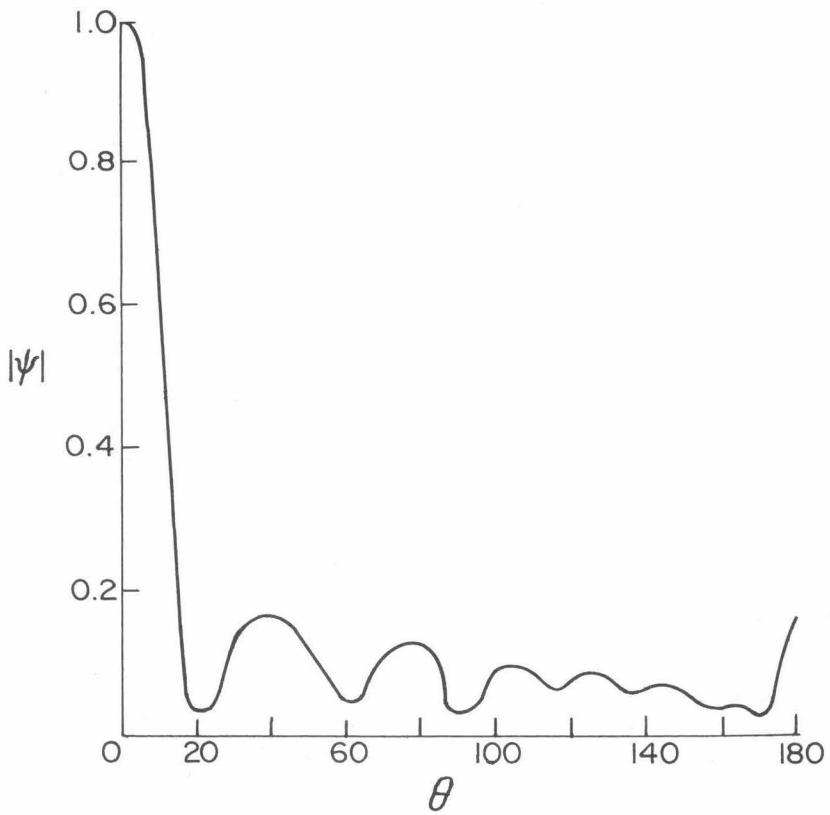

The far zone directional pattern for a 40^{o} cap combined with a 40^{o} - 45^{o} ring for ka = 14.2. The amplitude of vibration of the cap is 1/3 that of the ring and the two elements are 180^{o} out of phase.

Fig. 13

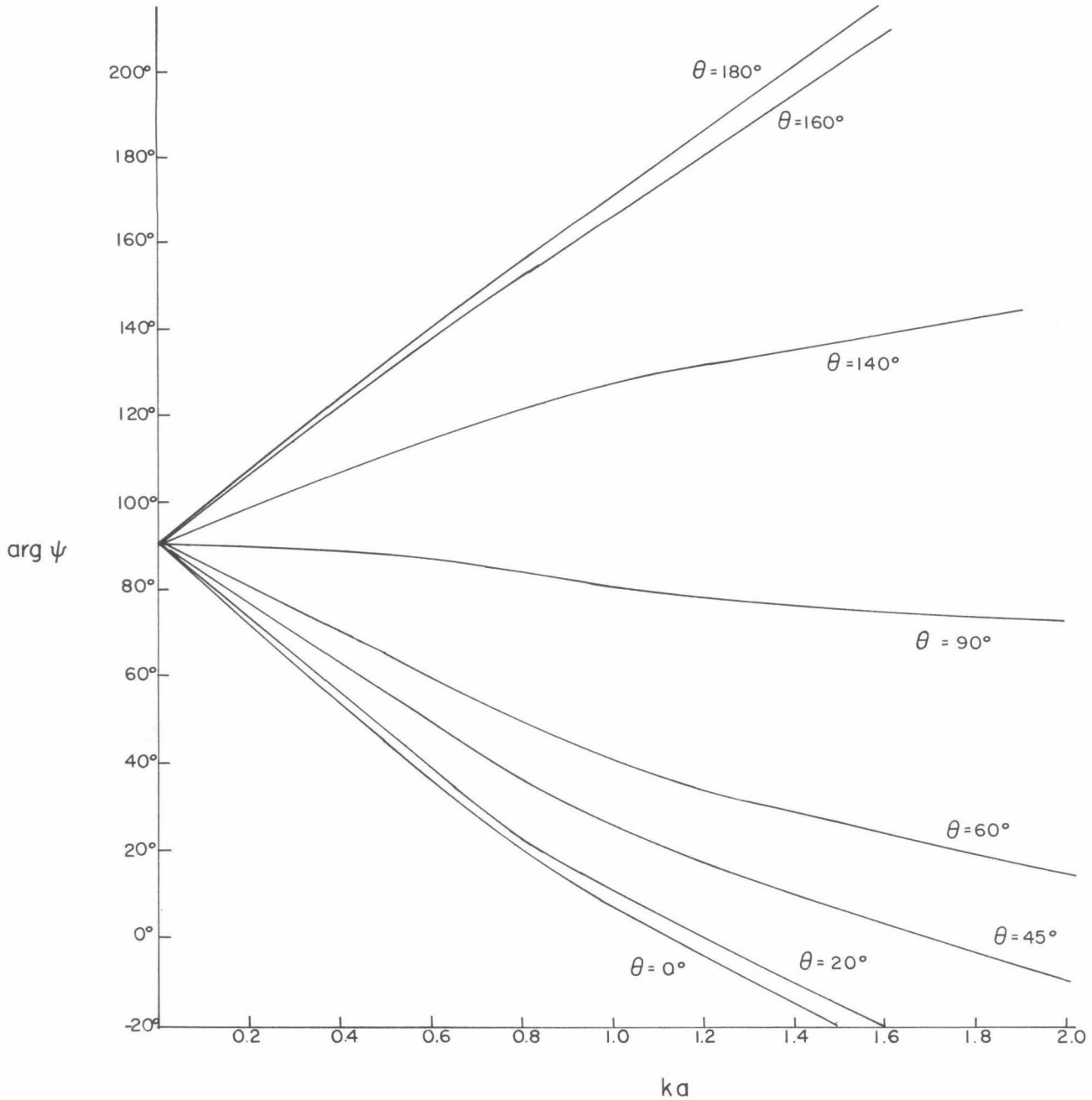

The phase of the far zone pressure field of a point source as a function of frequency in the lower frequency range.

Fig. 14

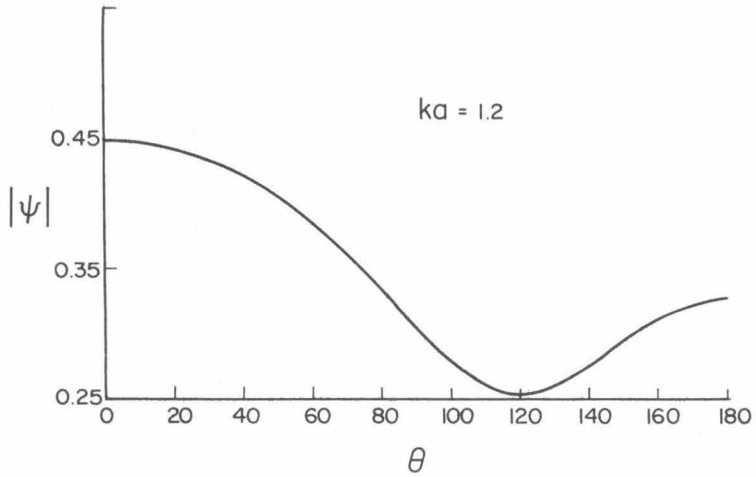

(a) The far zone pressure amplitude as a function of θ due to a point source at a frequency corresponding to ka = 1.2.

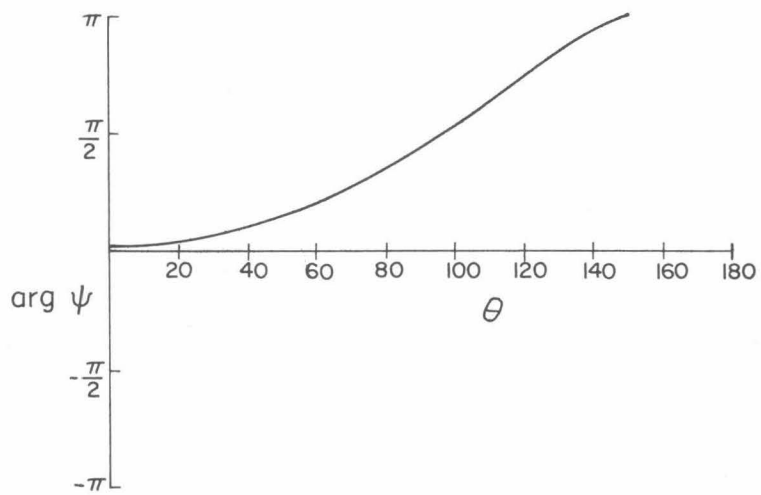

(b) The phase of the far zone pressure field as a function of θ due to a point source at a frequency corresponding to ka = 1.2.

Fig. 15

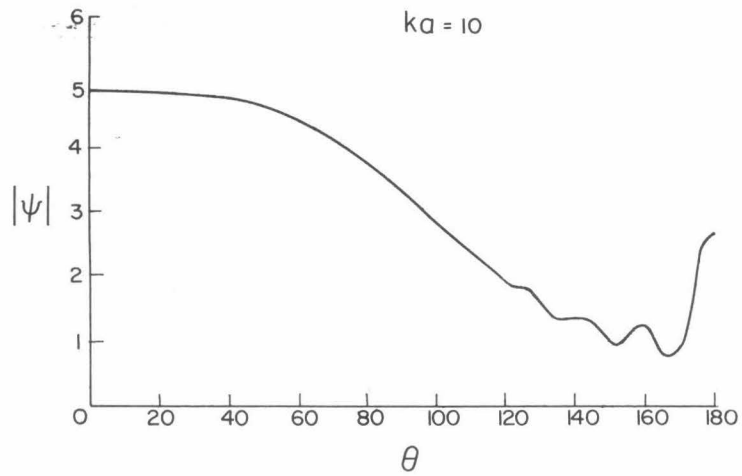

(a) The far zone pressure amplitude as a function of θ due to a point source at a frequency corresponding to ka = 10.

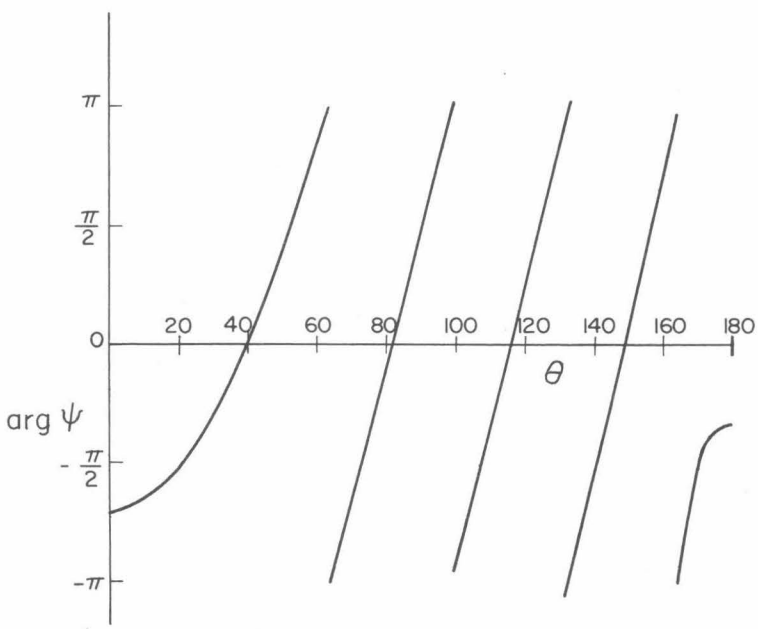

(b) The phase of the far zone pressure field as a function of θ due to a point source at a frequency corresponding to ka = 10.

Fig. 16

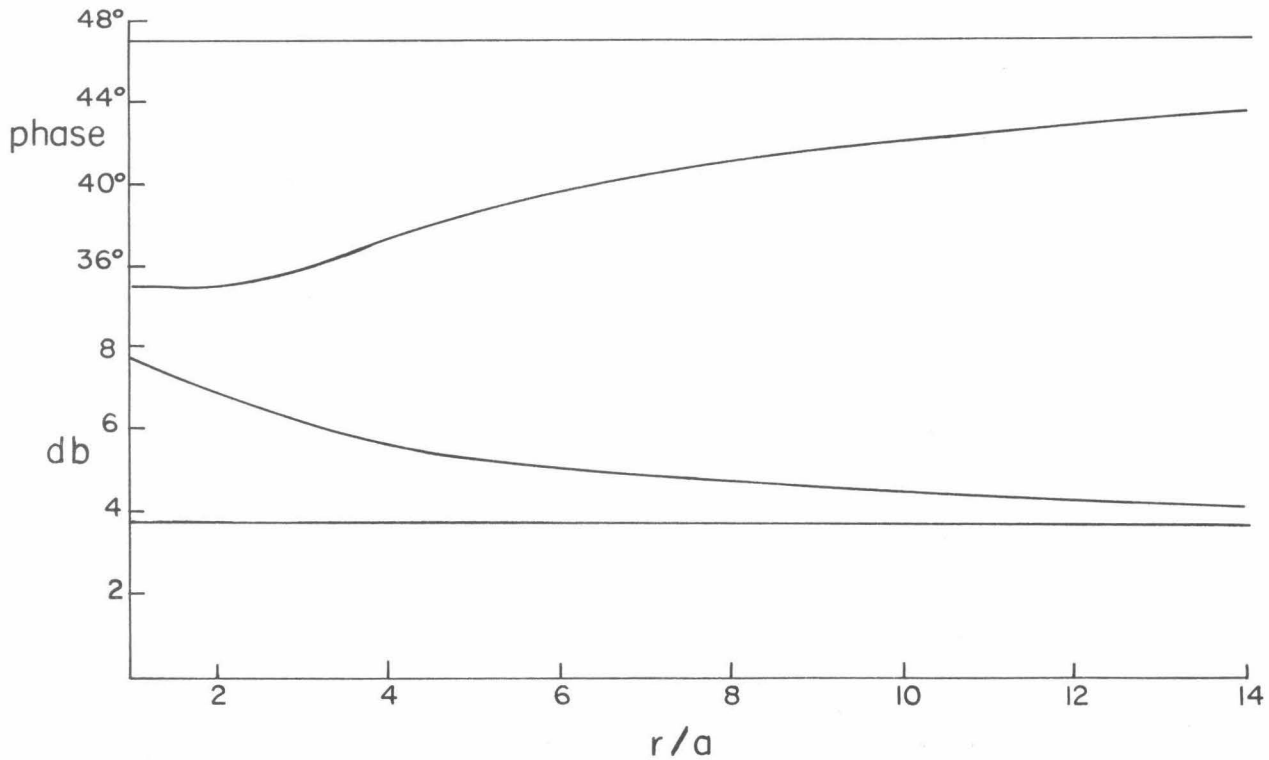

The phase and intensity difference between the two ears as a function of distance, for a point source situated 15° from the line of sight at a frequency corresponding to about 6 k/cs.

Fig. 17

DISTRIBUTION LIST FOR UNCLASSIFIED REPORTS ON CAVITATION

Contract Nonr-220(28)

Chief of Naval Research
Navy Department
Washington 25, D.C.
Attn: Code 438 (3)
Code 463 (1)

Commanding Officer
Office of Naval Research
Branch Office
The John Crerar Library Bldg.
86 E. Randolph Street
Chicago 1, Ill. (1)

Commanding Officer
Office of Naval Research
Branch Office
346 Broadway
New York 13, N.Y. (1)

Commanding Officer
Office of Naval Research
Branch Office
1030 E. Green Street
Pasadena 1, California (1)

Commanding Officer
Office of Naval Research
Navy 100, Fleet Post Office
New York, N. Y. (25)

Director
Naval Research Laboratory
Washington 25, D.C.
Attn: Code 2021 (6)

Chief, Bureau of Aeronautics
Navy Department
Washington 25, D.C.
Attn: Research Division (1)
Aero and Hydro Branch
(code Ad-3) (1)
Appl. Mech. Branch
(Code DE-3) (1)

Commander
Naval Ordnance Test Station
Inyokern, China Lake, Calif.
Attn: Technical Library (1)

Commander
Naval Ordnance Test Station
3202 E. Foothill Blvd.
Pasadena, California
Attn: Head, Underwater Ord. (1)
Head, Research Div. (1)

Chief, Bureau of Weapons
Navy Department
Washington 25, D.C.
Attn: Asst. Chief for Research
(Code Re) (1)
Systems Director, Underwater Ord. (Code Rexc) (1)
Armor, Bomb, Projectile, Rocket, Guided Missile Warhead and Ballistics Branch
(Code Re3) (1)
Torpedo Branch (Code Re6) (1)
Research and Components Section (Code Re6a) (1)
Mine Branch (Code Re7) (1)

Chief, Bureau of Ships
Navy Department
Washington 25, D.C.
Attn: Research and Development
(Code 300) (1)
Ship Design (Code 410) (1)
Preliminary Design and Ship Protection (Code 420) (1)
Scientific, Structural and Hydrodynamics (Code 442) (1)
Submarines (Code 525) (1)
Propellers and Shafting
(Code 554) (1)

Chief, Bureau of Yards and Docks, Navy Department
Washington 25, D.C.
Attn: Research Division (1)

Commanding Officer and Director
David Taylor Model Basin
Washington 7, D.C.
Attn: Hydromechanics Lab. (1)
Seaworthiness and Fluid Dynamics Div. (1)
Library (1)

Commanding Officer
Naval Ordnance Laboratory
White Oak, Maryland
Attn: Underwater Ord. Dept. (1)

Commanding Officer
Naval Underwater Ordnance Station
Newport, Rhode Island (1)

Director
Underwater Sound Laboratory
Fort Trumbull
New London, Connecticut (1)

Librarian
U.S. Naval Postgraduate School
Monterey, California (1)

Executive Secretary
Research and Development Board
Department of Defense
The Pentagon
Washington 25, D.C. (1)

Chairman
Underseas Warfare Committee
National Research Council
2101 Constitution Avenue
Washington 25, D.C. (1)

Dr. J. H. McMillen
National Science Foundation
1520 H Street, N.W.
Washington, D.C. (1)

Director
National Bureau of Standards
Washington 25, D.C.
Attn: Fluid Mechanics Section (1)

Dr. G. H. Keulegan
National Hydraulic Laboratory
National Bureau of Standards
Washington 25, D.C. (1)

Director of Research
National Aeronautics and
Space Administration
1512 H Street, N.W.
Washington 25, D.C. (1)

Director
Langley Aeronautical Laboratory
National Aeronautics and Space Admin.
Langley Field, Virginia (1)

Mr. J. B. Parkinson
Langley Aeronautical Laboratory
National Aeronautics and Space Admin.
Langley Field, Virginia (1)

Commander
Air Research and Development
Command
P.O. Box 1395
Baltimore 18, Maryland
Attn: Fluid Mechanics Div. (1)

Director
Waterways Experiment Station
Box 631
Vicksburg, Mississippi (1)

Beach Erosion Board
U.S. Army Corps of Engineers
Washington 25, D.C. (1)

Office of Ordnance Research
Department of the Army
Washington 25, D.C. (1)

Office of the Chief of Engineers
Department of the Army
Gravelly Point
Washington 25, D.C. (1)

Commissioner
Bureau of Reclamation
Washington 25, D.C. (1)

Director
Oak Ridge National Laboratory
P.O. Box P
Oak Ridge, Tenn. (1)

Sandia Corporation Library
Sandia Base
Albuquerque, New Mexico (1)

Professor Carl Eckart
Scripps Institute of Oceanography
La Jolla, California (1)

Documents Service Center
Armed Services Technical
Information Agency
Arlington Hall Station
Arlington 12, Virginia (10)

Mr. Wing G. Agnew, Chief
Spokane Field Office, Region I
U.S. Dept. of the Interior
Bureau of Mines
1201 N. Division Street
Spokane 2, Washington (1)

Office of Technical Services
Department of Commerce
Washington 25, D.C. (1)

Polytechnic Institute of Brooklyn
Department of Aeronautical
Engineering and Applied Mech.
99 Livingston Street
Brooklyn 1, New York
Attn: Prof. H. Reissner (1)

Division of Applied Mathematics
Brown University
Providence 12, Rhode Island (1)

California Institute of Technology
Pasadena 4, California
Attn: Professor A. J. Acosta (1)
Professor A. Hollander (1)
Professor C. B. Millikan (1)
Professor M. S. Plesset (1)
Professor V. A. Vanoni (1)
Professor T. Y. Wu (1)

University of California
Department of Engineering
Berkeley 4, California
Attn: Professor H. A. Einstein (1)
Professor H. A. Schade (1)
Professor J. V. Wehausen (1)

Case Institute of Technology
Dept. of Mechanical Engineering
Cleveland, Ohio
Attn: Professor G. Kuerti (1)

Cornell University
Grad. School of Aeronautical
Engineering
Ithaca, New York
Attn: Prof. W. R. Sears (1)

Harvard University
Cambridge 38, Mass.
Attn: G. Birkhoff, Dept. of
Mathematics (1)
G. Carrier, Div. of
Eng. and Appl. Physics (1)

University of Illinois
Dept. of Theoretical and Applied
Mechanics
College of Engineering
Urbana, Illinois
Attn: Dr. J. M. Robertson (1)

State University of Iowa
Iowa Institute of Hydraulic
Research
Iowa City, Iowa
Attn: Dr. Hunter Rouse (1)

University of Maryland
Inst. for Fluid Dynamics and
Applied Mathematics
College Park, Maryland
Attn: Prof. M. H. Martin (1)
Prof. J. R. Weske (1)

Massachusetts Institute of
Technology
Cambridge 39, Mass.
Attn: Prof. W. M. Rohsenow,
Dept. Mech. Engr. (1)
Prof. A. T. Ippen
Hydrodynamics Laboratory (1)

Michigan State College
Hydraulics Laboratory
East Lansing, Michigan
Attn: Prof. H. R. Henry (1)

University of Michigan
Ann Arbor, Michigan
Attn: Director, Engineering Re-
search Institute (1)
Prof. V. L. Streeter,
Civil Engineering Dept. (1)

University of Minnesota
St. Anthony Falls Hydraulic Lab.
Minneapolis 14, Minn.
Attn: Dr. L. G. Straub (1)

New York University
Institute of Mathematical Sciences
25 Waverly Place
New York 3, New York
Attn: Prof. R. Courant (1)

University of Notre Dame
College of Engineering
Notre Dame, Indiana
Attn: Dean K. E. Schoenherr (1)

Pennsylvania State University
Ordnance Research Laboratory
University Park, Pennsylvania
Attn: Prof. G. F. Wislicenus (1)

Dr. J. Kotik
Technical Research Group
2 Aerial Way
Syosset, New York (1)

Professor H. Cohen
IBM Research Center
P.O. Box 218
Yorktown Heights, New York (1)

Stanford University
Stanford, California
Attn: Prof. D. Gilbarg, Dept. of Mathematics (1)
Prof. L. I. Schiff, Dept. of Physics (1)
Prof. J. K. Vennard, Dept. of Civil Eng. (1)

Stevens Institute of Technology
Experimental Towing Tank
711 Hudson Street
Hoboken, New Jersey (1)

Worcester Polytechnic Institute
Alden Hydraulic Laboratory
Worcester, Mass.
Attn: Prof. J. L. Hooper (1)

Dr. Th. von Karman
1051 S. Marengo Street
Pasadena, California (1)

Aerojet General Corporation
6352 N, Irwindale Avenue
Azusa, California
Attn: Mr. C. A. Gongwer (1)

Dr. J. J. Stoker
New York University
Institute of Mathematical Sciences
25 Waverly Place
New York 3, New York (1)

Prof. C. C. Lin
Dept. of Mathematics
Massachusetts Institute of Technology
Cambridge 39, Mass. (1)

Dr. Columbus Iselin
Woods Hole Oceanographic Inst.
Woods Hole, Mass. (1)

Dr. A. B. Kinzel, Pres.
Union Carbide and Carbon Research Laboratories, Inc.
30 E. 42nd Street
New York, N. Y. (1)

Dr. F. E. Fox
Catholic University
Washington 17, D.C. (1)

Dr. Immanuel Estermann
Office of Naval Research
Code 419
Navy Department
Washington 25, D.C. (1)

Goodyear Aircraft Corporation
Akron 15, Ohio
Attn: Security Officer (1)

Dr. F. V. Hunt
Director, Acoustics Research Laboratory
Harvard University
Cambridge, Mass. (1)

Prof. Robert Leonard
Dept. of Physics
University of California at Los Angeles
West Los Angeles, California (1)

Technical Librarian
AVCO Manufacturing Corp.
2385 Revere Beach Parkway
Everett 49, Mass. (1)

Dr. L. Landweber
Iowa Inst. of Hydraulic Research
State University of Iowa
Iowa City, Iowa (1)

Dr. M. L. Ghai, Supervisor
Heat Transfer/Fluid Mechanics
Rocket Engine-Applied Research
Building 600
Aircraft Gas Turbine Division
General Electric Company
Cincinnati 15, Ohio (1)

Dr. W. W. Clauson
Rose Polytechnic Institute
R.R. No. 5
Terre Haute, Indiana (1)

Mr. Kurt Berman
Rocket Engine Section
Aircraft Gas Turbine
Development Dept.
Malta Test Station
Ballston Spa, New York (1)

Officer in Charge
MWDP Contract Supervisory Staff
SACLANT ASW Research Center
APO 19, New York, N. Y. (1)

Hydronautics, Incorporated
200 Monroe Street
Rockville, Maryland
Attn: Mr. Phillip Eisenberg
Mr. Marshall P. Tulin (1)

Commanding Officer and Director
U.S. Naval Civil Engineering Lab.
Port Hueneme, California
Attn: Code L54 (1)

Dr. H. L. Uppal, Director
Irrigation and Power Research
Institute
Punjab, Amritsar, India (1)

Prof. Taizo Hayashi, Director
Hydraulics Laboratory
Chuo University
1, 1-chome, Koishikawa-mati
Bunkyo-ku, Tokyo, Japan (1)

Prof. J. E. Cermak
Department of Civil Engineering
Colorado State University
Fort Collins, Colorado (1)

Mr. John P. Herling
Order Librarian
Engineering Societies Library
United Engineering Trustees, Inc.
29 West 39th Street
New York 18, N. Y. (1)

Mr. R. W. Kermeen
Dept. 8173, Bldg. 181N
Lockheed Aircraft Corp.
Missiles and Space Division
P.O. Box 504, Sunnyvale, Cal. (1)

Material Laboratory Library
Building 291, Code 912B
New York Naval Shipyard
Brooklyn 1, New York (1)

Professor Frederick G. Hammitt
Nuclear Engineering Department
The University of Michigan Re-
search Institute
Ann Arbor, Michigan